Z. Phys. A 351, 333–344 (1995)

ZEITSCHRIFT
FÜR PHYSIK A

K^--meson production in proton-nucleus collisions

A. Sibirtsev[1,*], M. Büscher[2], H. Müller[1], Ch. Schneidereit[1]

[1] Institut für Kern- und Hadronenphysik, Forschungszentrum Rossendorf, Postfach 510119, D-01314 Dresden, Germany**
[2] Institut für Kernphysik, Forschungszentrum Jülich, D-52425 Jülich, Germany

Received: 19 October 1994

Abstract. K^--meson production in proton-nucleus interactions at projectile energies up to 15 GeV is studied. As a first step the available data on K^--meson production in pp interactions are compared with different parametrizations and results of model calculations. Because of considerable uncertainties in the current descriptions of the energy dependence of the elementary K^- cross section a new parametrization is suggested. Experimental data on K^- production in pA collisions are analyzed in the framework of the Rossendorf-Collision and folding models. Satisfactory descriptions of the momentum spectra at forward angles are achieved. From an analysis of the A dependence it can be concluded that K^- mesons are well suited to investigate final-state interactions for particles interacting strongly with the residual nucleus. Furthermore, we propose experimental studies on K^- production close to threshold. Such measurements are particularly sensitive to contributions from secondary processes or from multi-nucleon interactions.

PACS: 25.40.Ve; 25.10.+s; 25.90.+k

1. Introduction

The study of strange-particle production in proton-nucleus (pA) and nucleus-nucleus (AA) collisions has attracted considerable attention during the last decade. More than ten years ago strangeness enhancement and K^+ destillation were predicted theoretically by Rafelski and Müller [1] and Greiner et al. [2]. Their calculations were based on the picture that nuclear matter, which consists primarily of u and d quarks at normal density ρ_0, melts into a "soup" of quarks and gluons at high baryon density. The Fermi energy E_F of this "soup" increases with the density ρ and reaches values of about 430 MeV at high densities $\rho \approx 10\rho_0$. Under such conditions $s\bar{s}$ creation is no longer suppressed and nearly equal amounts of $s\bar{s}$ as well as $u\bar{u}$ and $d\bar{d}$ pairs are produced. This simple picture is the general basis for the theoretical prediction on enhancement of strangeness production in nuclear reactions at high baryon density.

The $s\bar{s}$ pairs created in the "soup" containing u and d quarks may form $K^+(\bar{s}u)$, $K^0(\bar{s}d)$ mesons and $\Lambda(uds)$, $\Sigma(uus, uds$ or $dds)$ hyperons, whereas the rate for $K^-(\bar{u}s)$ production is suppressed because of the necessity to create additional $u\bar{u}$ pairs. Thus, the K^+/K^- ratio is a sensitive probe for high-density quark matter and seems to be a reasonable tool for the detection of the quark-gluon plasma.

In the experimental studies on strangeness production in heavy-ion collisions at high energies performed by E802 [3], NA34 [4] and NA35 [5] $s\bar{s}$ creation has in fact been observed to be about three times larger than in free pp collisions. The strangeness is carried mainly by Λ, Σ hyperons and K^+, K^0 mesons, whereas a negligible fraction of K^- mesons is produced. Although these experimental data reasonably agree with theoretical predictions based on the quark-gluon plasma hypothesis, there are other experimental findings which do not fit into the quark-gluon scenario. For pBe, pAu and SiAu collisions at 14.6 GeV/u the E802 collaboration [3] found a constant K^+/K^- ratio for an increasing size of the interacting system in contrast to the predicted K^- suppression. Thus, the quark-gluon hypothesis needs further confirmation. In particular, it has to be investigated if other reaction mechanisms can be responsible for the enhancement of strange-particle production in heavy-ion collisions.

An alternative description of strangeness production is based on a conventional collision picture and includes mainly two reaction mechanisms. Particularly, for K^+-meson production the one-step reaction

$$N + N \rightarrow K^+ + X \tag{1}$$

and the two-step process

$$N + N \rightarrow \pi + X,\ \pi + N \rightarrow K^+ + X \tag{2}$$

and for K^--meson production the analogous processes

$$N + N \rightarrow K^- + X \tag{3}$$

and

$$N + N \rightarrow \pi + X,\ \pi + N \rightarrow K^- + X \tag{4}$$

* *Permanent address:* Institute of Theoretical and Experimental Physics, Cheremushkinskaya 25, 117259 Moscow, Russia
** Supported by the Bundesministerium für Forschung und Technologie, Germany

are usually considered. Contributions from the two-step processes (2) and (4) are often discussed to be significant even at high bombarding energies. In spite of the fact that the cross section for strangeness production in pion-induced reactions is small ($\sim$1 mb for K^+ and $\sim$0.1 mb for K^-), the pion multiplicity is large enough to lead to a significant contribution to K^- production via these mechanisms. As was pointed out by Stachel [6] and Nagamiya [7], such a contribution from secondary processes might be strong enough to prevent the observation of the quark-gluon plasma.

Although the significance of secondary processes is generally accepted, a quantitative understanding needs further experimental and theoretical studies. At pion momenta below 2 GeV/c the cross sections of $\pi N \rightarrow K^+X$ and $\pi N \rightarrow K^-X$ reactions are rather large. Therefore, pA collisions in the few-GeV region, where pions in this momentum range are produced, are well suited to determine the maximum possible contribution from the secondary reaction channels (2) and (4). Such experiments on K^+ production in pp and pA collisions have been proposed for the proton synchrotron COSY [8, 9] and the ITEP facility [10].

So far, several theoretical articles on K^+ production in proton-induced reactions have been published. It was shown by Cassing et al. [11] and Sibirtsev and Büscher [12] that the two-step reaction mechanism (2) dominates below the free nucleon-nucleon threshold of T_{th} = 1.58 GeV. As was discussed by Müller and Sistemich [13], at interaction energies far below T_{th} even the role of collisions with several target nucleons becomes significant. At bombarding energies above 1.6 GeV the direct kaon production (1) was found to be dominant [11, 12, 14].

The study of K^- production is even more attractive in view of the fact that there are no reliable and consistent studies of K^--production cross sections. Therefore, further experimental and theoretical work must be done in order to understand the $s\bar{s}$ creation dynamics. As a first step it must be investigated whether the available data on pA collisions can be understood in terms of a standard hadronic scenario. Then the analysis should be extended to heavy-ion interactions.

In this paper experimental data on K^- production in pA collisions are analyzed and the possible reaction mechanisms are discussed. To evaluate the contribution from the direct process (3) the cross section of the elementary reaction $pp \rightarrow K^-X$ is calculated and the results are compared with available experimental data. The dependence of the K^- yield on the bombarding energy in pA collisions as well as the A dependence are discussed. Final-state interactions (FSI) of K^- mesons with the residual nucleus are explored in order to evaluate the dependence of the reabsorption probability on the size of the interacting system. Some features of the experimental study of K^--meson production in pA collisions close to the threshold are discussed, the energy dependence of K^--meson yields down to subthreshold energies and spectra for an incident proton energy of 2.5 GeV are predicted. In order to make these predictions more reliable two different models are used.

2. K^- production in pp collisions

In the framework of folding models (see Sect. 3) one of the most important ingredients for the calculation of K^- production in pA and AA collisions is the cross section of the elementary reaction (3). For the understanding of subthreshold production of K^- mesons the energy dependence of the elementary cross section down to the lowest energies is of special interest. Unfortunately, in the near-threshold region there are not enough data available to determine this energy dependence with the desired accuracy.

In Fig. 1 the present situation is visualized. All available experimental data are plotted as a function of $s - s_{\mathrm{th}}$ with $s = 2m_p(2m_p + T_p)$ being the square of the invariant energy and $s_{\mathrm{th}} = 4(m_p + m_K)^2$ the corresponding threshold energy. The mass and the kinetic energy of the proton are denoted by m_p and T_p, the mass of the K^- meson by m_K.

The cross section at the lowest energy (2.85 GeV) is of special importance for the extrapolation to lower energies. A value of $\sigma_{K^-} \simeq (4 \pm 2)\,\mu$b was obtained by Reed et al. [15] from a measurement of the differential cross section for 1.1 GeV/c K^- mesons at an angle of 0°. It should be noted that the cross section was deduced by an integration over momentum and angle assuming a homogeneous distribution in phase-space. In another experiment [16] on production of strange particles at the same energy one event of K^+K^--pair production was observed indicating $\sigma_{K^-} < 10\,\mu$b, which does not contradict the result of [15]. K^--production cross sections in the region 3 GeV^2 $< s - s_{\mathrm{th}} <$10 GeV^2 were obtained by Efremov and Paryev [17] by summing the partial cross sections from compilation [18] and applying charge symmetry invariance to K^- and $\overline{K^0}$ mesons. The data at higher energies were taken from the review of Giacomelli [19].

A first attempt to parametrize the antikaon-production cross section was made by Zwermann and Schürmann [20] about a decade ago. Assuming that the cross section is the same for protons and neutrons, for K^+ and K^0 and for K^- and $\overline{K^0}$, respectively, they suggested

$$\sigma_{K^-} = 25 \left(\frac{p^*_{\mathrm{max}}}{\mathrm{GeV/c}} \right) \ \mu\mathrm{b} \ , \tag{5}$$

where p^*_{max} is the maximum CM momentum of the outgoing kaons from $NN \rightarrow NNK\overline{K}$ reactions. This parametrization was in fair agreement with the available data only in the energy region from about 3 to 10 GeV^2 and was used to extrapolate to lower energies. However, for energies $s - s_{\mathrm{th}} < 3$ GeV^2 Parametrization (5) (dashed line in Fig. 1) is in strong disagreement with a recent parametrization (dotted line) of the inclusive K^--production cross section suggested by Efremov and Paryev [17]

$$\sigma_{K^-} = \left(\frac{s/s_{\mathrm{th}} - 1}{s/s_{\mathrm{th}}} \right)^3 \times \sum_{i=1}^{3} a_i F_i(s/s_{\mathrm{th}}) \ . \tag{6}$$

In (6) the parameters a_i were adjusted to the available experimental data and the functions F_i were taken from [21].

A disadvantage of the fitting procedures (5) and (6) is related to the fact that most of the available experimental data were obtained at rather high energies. An extrapolation down to lower energies is necessary for a calculation of

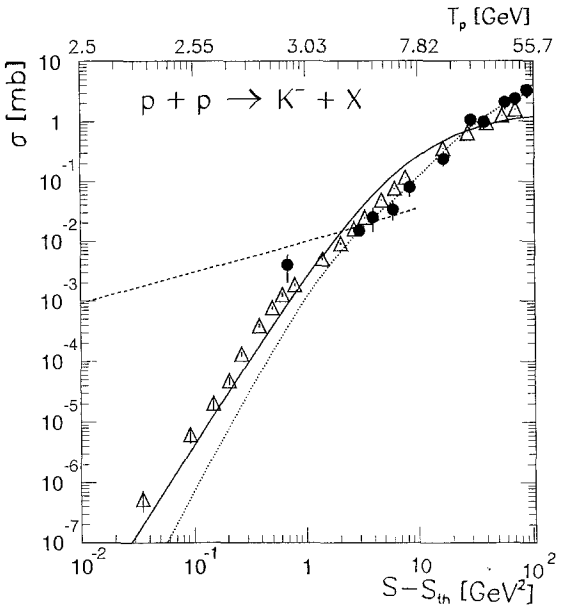

Fig. 1. Total K^--production cross section in pp collisions as a function of the available energy $s - s_{\rm th}$. The experimental data (*full circles*) are compared with the ROC-model results (*triangles*) and Parametrizations (5) (*dashed line*) and (6) (*dotted line*). The *solid line* represents the fit (7) to the ROC-model calculations

subthreshold production in pA and AA collisions. Such an extrapolation is always connected with large uncertainties. We attempt to resolve these ambiguities by calculating the K^--production cross section at low energies using an improved version of the model [22] developed in Rossendorf to describe hadronic and nuclear interactions. In the following it is referred to as the ROC (ROssendorf Collision) model.

In the framework of the ROC model pp collisions proceed via the excitation and subsequent decay of the interacting particles. The excited states can be viewed as systems consisting of the valence quarks of the incoming particles as well as an arbitrary number of $q\bar{q}$ pairs. The production of $s\bar{s}$ pairs is suppressed relative to that of $u\bar{u}$ and $d\bar{d}$ pairs according to the ratio $u : d : s = 1 : 1 : \lambda$. For the strangeness-suppression factor a value of λ=0.15 was taken following the analysis of strange-particle production by Wroblewski [23]. The model reasonably reproduces experimental data on p, π, K, $\overline{K}$ and hyperon production in pp collisions at energies from threshold to about 12 GeV [22, 24] using a fixed energy-independent set of parameters. Especially the recently demonstrated [24] ability of the ROC model to reproduce various particle production channels down to the thresholds gives confidence concerning the reliability of the results on K^- production near the threshold.

From Fig. 1 it can be seen that the results from the ROC-model calculations (triangles) satisfactorily describe the available data. In the low-energy region they lie between the Parametrizations (5) and (6). The disagreement between (5) on the one hand and Parametrization (6) and ROC-model results on the other hand is a crucial point for the interpretation of the experimental results obtained by Shor et al. [25] on subthreshold production of K^- mesons in AA collisions at 2.1 GeV/u. Zwermann and Schürmann [20] conclude from their calculations that the creation of K^- mesons via a sequence of independent baryon-baryon collisions is the dominant mechanism in heavy-ion reactions at subthreshold energies. The same conclusion was obtained recently by Li et al. [26] from an analysis of K^- production in NiNi collisions at 1.85 GeV/u. In the light of the results presented here their conclusions should be considered with caution because (5) obviously overestimates the elementary K^--production cross section at low energies.

Using the ROC-model calculations as the presently most reliable result in the near threshold region a new parametrization

$$\sigma_{K^-} = 1.5 \times (1.0 - s_{\rm th}/s)^{2.9} \ \text{mb} \ , \tag{7}$$

which is shown as a solid line in Fig. 1, is proposed for further use in theoretical works on K^- production in nuclear reactions.

3. Models for K^- production in pA collisions

To calculate K^- production in proton-nucleus collisions two different models, the folding and the ROC model, are used. In the following the principal assumptions as well as similiarities and differences of the two approaches are briefly described.

3.1. The folding model

A justification of the folding model and a comparison with experimental data can be found in the publications of Cassing et al. [27], Sibirtsev [28] and references therein. The model reasonably reproduces available experimental results on η and K^+ production in pA collisions.

We analyze the direct K^- production in pA collisions using the standard reaction mechanisms. In the framework of the first-collision model the K^- meson is produced via reaction (3) in an interaction of the incident proton with a target nucleon. The invariant differential cross section is given as

$$E_{K^-}\frac{{\rm d}^3\sigma_{K^-}}{{\rm d}\mathbf{p}_{K^-}} = N_{\rm eff}(A)\kappa(p_{K^-}, A) \int \Phi(\mathbf{q}) E^*_{K^-}\frac{{\rm d}^3\sigma_{pN\to K^-X}(s)}{{\rm d}\mathbf{p}^*_{K^-}}{\rm d}\mathbf{q} \ , \tag{8}$$

where $\Phi(\mathbf{q})$ is the relative momentum function, which describes the distribution of the internal momentum $\mathbf{q}$ of the nucleons. It is taken according to the standard Fermi-gas model [28]. The factor $N_{\rm eff}$, the effective number of nucleons participating the interaction, was calculated by the Glauber approach [29] and $\kappa(p_{K^-}, A)$, the antikaon reabsorption factor, will be discussed in Sect. 4. Momentum and energy of the produced K^- meson in the pN rest system are denoted by $\mathbf{p}^*_{K^-}$ and $E^*_{K^-}$. The squared invariant energy of the incident proton-nucleon (pN) system is given by $s = (E_p + m_N)^2 - (\mathbf{p}_p + \mathbf{q})^2$, where $E_p, \mathbf{p}_p$ and m_N are the total energy and momentum of the incident proton and the nucleon mass, respectively. Note that we take into account the off-shell behaviour of the nucleons by using their on-shell mass instead of their total energy in the formula. In (8), $E{\rm d}^3\sigma_{pN\to K^-X}(s)/{\rm d}\mathbf{p}_{K^-}$ stands for the elementary differential K^--production cross section in free pN collisions.

Following Taylor et al. [30] and Johnson et al. [31] the elementary invariant cross section for inclusive single-particle production may be written as a function of three variables: the transverse momentum p_t, the radial scaling variable x_R and the squared invariant energy s. The variable x_R is defined as $x_R = E^*/E^*_{max}$, where E^* is the energy and E^*_{max} the maximum energy of the detected particle in the CM system. Assuming factorization in p_t and x_R space the inclusive cross section can be written as

$$\frac{d^3\sigma_{pN\to K^-X}(s,p_t,x_R)}{dp_{K^-}} = \sigma_{K^-} \times f_1(p_t) \times f_2(x_R) , \qquad (9)$$

where σ_{K^-} denotes the total production-cross section for which Parametrization (6) is used in the following calculations. In [17] a p_t dependence

$$f_1(p_t) = \exp\left(b - \sqrt{b^2 + c(s)p_t^2}\right) \qquad (10)$$

was suggested with slope $b = \sqrt{3}$ and the parameter $c(s)$ adjusted to experimental data

$$c(s) = (0.29 \pm 0.15)(s - s_{th})^{(0.85\pm0.06)}. \qquad (11)$$

At energies $s - s_{th} < 1$ GeV^2 the K^- production is almost isotropic and $f_1(p_t) \simeq$ const.. The dependence on the radial scaling variable x_R was taken in accordance with [30, 31]

$$f_2(x_R) = (1 - x_R)^{n(s)}. \qquad (12)$$

Close to the reaction threshold the x_R distribution is governed by the phase space and $n(s) \simeq 2$. At energies above $s \simeq 100$ GeV^2 the average value of $n(s) = 5.5 \pm 0.7$ was obtained from an analysis of the experimental data [19, 30, 31]. According to the quark-parton model a value of $n(s) = 7$ is expected for K^- mesons in the relativistic regime. In agreement with this energy dependence we suggest the following parametrization

$$n(s) = (2.2 \pm 0.1)(s - s_{th})^{(0.15\pm0.02)}. \qquad (13)$$

At energies $s - s_{th} < 1$ GeV^2 phase-space distributions were used for proton-nucleus calculations instead of (9).

To analyze strangeness production in nuclear reactions we also take into account the secondary process (4). The K^--production cross section in the two-step reaction mechanism is expressed by

$$E_{K^-}\frac{d^3\sigma_{K^-}}{dp_{K^-}} = N_{eff}(A)\ \kappa(p_{K^-}, A) \int\int \Phi(\mathbf{q}) F(\mathbf{p}_\pi) W(\mathbf{p}_\pi, A)\ E^*_{K^-}\frac{d^3\sigma_{\pi N\to K^-X}(s)}{dp^*_{K^-}} d\mathbf{q} d\mathbf{p}_\pi , \qquad (14)$$

where the probability $W(\mathbf{p}_\pi, A)$ for the produced pions to interact with a target nucleon is calculated in accordance with [11].

The pion spectrum $F(\mathbf{p}_\pi)$ is calculated in the framework of the first-collision model as

$$F(\mathbf{p}_\pi) = \int \Phi(\mathbf{q}) E^*_\pi \frac{d^3\sigma_{pN\to\pi X}(s)}{dp^*_\pi}\frac{1}{\sigma^{tot}_{pN}} d\mathbf{q} , \qquad (15)$$

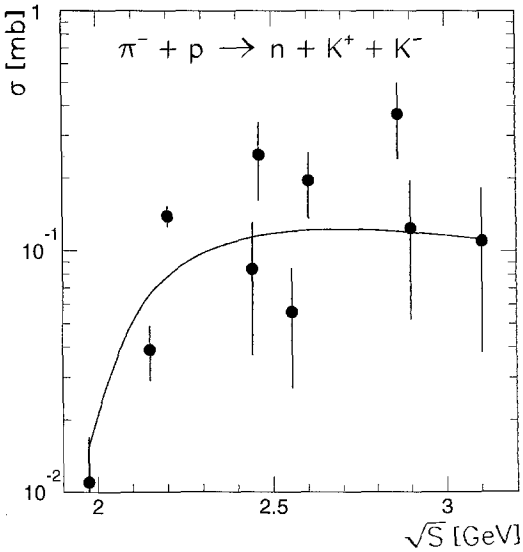

Fig. 2. K^--production cross section in π^-p reaction as a function of $\sqrt{s}$. Experimental data (circles) are from [18], the solid line represents Parametrization (16)

with $E_\pi d^3\sigma_{pN\to\pi X}(s)/dp_\pi$ being the elementary pion cross section and σ^{tot}_{pN} the total proton-nucleon cross section. The total pion-production cross section is taken from the compilation of experimental data by Flaminio et al. [18] and the differential cross section is assumed to be isotropic in the pN rest system and completely determined by energy and momentum conservation.

The total K^--production cross section in pion-nucleon collisions is described by the function

$$\sigma(\pi + N \to N + K^+ + K^-) = \frac{A(\sqrt{s} - \sqrt{s_{th}})}{B^2 + (\sqrt{s} - \sqrt{s_{th}})^2} , \qquad (16)$$

with parameters $A = 0.188$ mb GeV and $B = 0.767$ GeV obtained from the analysis of the reaction $\pi^- + p \to n + K^+ + K^-$. In Fig. 2 we compare Parametrization (16) with the experimental data from [18]. The differential cross section of this reaction is deduced from phase-space considerations.

3.2. The Rossendorf Collision Model

In the framework of the ROC model hadron-hadron, hadron-nucleus and nucleus-nucleus collisions are treated in a unified way on the basis of the same assumptions and principles. The model is implemented as a Monte-Carlo generator which samples complete events. In this way, all final channels and all interesting physical quantities can be considered simultaniously.

A pA reaction is treated as a superposition of NN interactions. Each event is characterized by the number l of target nucleons involved in the reaction. The cross sections σ_{1l} for the interaction of the projectile with l target nucleons are calculated on the basis of a probabalistic interpretation of the Glauber theory [29]. A multi-step picture is proposed to describe the interaction process, where a group of l participating target nucleons is treated as a single entity called cluster. In the first step translational energy is converted into

internal excitation energy of the projectile, the cluster and the residual nucleus consisting of $L = A - l$ nucleons.

The excited projectile- and cluster-like states contain the valence quarks of the initial nucleons. During the collision further quark-antiquark pairs can be created which, in the second stage of the reaction, recombine randomly with the valence quarks building up baryons and mesons in accordance with the rules of quark statistics [32]. Primarily produced resonances decay in further steps into stable hadrons. Analogously, the de-excitation of a cluster results in the production of baryons and mesons and may, in addition, lead to the emergence of light fragments such as deuterons, tritons and so on. Since the structure of the residual nucleus is disturbed by the projectile-cluster interaction, it becomes also excited and breaks into several fragments.

During the second stage of the reaction the channels $\alpha_{1lL} = (\alpha_1, \alpha_l, \alpha_L)$ are populated, which are defined by the numbers n_1, n_l, n_L and types of particles in the final states of the decaying projectile, cluster and residual nucleus, respectively. By introducing the relative probability $\mathrm{d}W_{1lL}(s;\alpha_{1lL})$ of populating the channel α_{1lL} the differential cross section is calculated as an incoherent sum

$$\mathrm{d}\sigma(s) = \sum_{l=1}^{A} \sigma_{1l} \sum_{\alpha_{1lL}} \mathrm{d}W_{1lL}(s;\alpha_{1lL}), \tag{17}$$

with A being the mass number of the target nucleus and s denoting the square of the CM energy of the projectile-target system. The cross sections σ_{1l} depend on the nucleon density in the target nucleus and on the elementary NN cross section σ_{NN}. For details concerning the calculation of σ_{1l} we refer to [33]. The quantities

$$\mathrm{d}W_{1lL}(s;\alpha_{1lL}) \propto \mathrm{d}R_n(s;\alpha_{1lL})A(\alpha_{1lL}) \tag{18}$$

describe the collision dynamics, the relative probabilities of the various channels and the distribution of the final particles in phase space. They are given by the Lorentz-invariant phase-space factor $\mathrm{d}R_n(s;\alpha_{1lL})$ of the n primarily produced final particles times $A(\alpha_{1lL})$, the square of the reaction matrix element.

The phase-space factor depends on the four-momenta of the projectile and the target nucleus in the initial state and on the masses of the n particles in the final state. The target nucleus is assumed to dissociate during the interaction into spectators and participants. Their relative momenta are described by the momentum distribution $\rho(\mathbf{p}_L)$, with $\mathbf{p}_L$ being the three-momentum of the residual nucleus. By decomposing the whole phase-space factor according to the recursion formulas of [34] the relative probability $\mathrm{d}W_{1lL}$ can be split into a factor arising from the Fermi motion, a term describing the interaction of the projectile with the participants and factors connected with excitation and decay of the projectile, the cluster and the residual nucleus

$$\mathrm{d}W_{1lL}(s;\alpha_{1lL}) \propto \frac{\mathrm{d}^3 p_L}{2e_L}\rho(\mathbf{p}_L)\mathrm{d}R_2(s';M_1,M_l)A_{sc}(t') \prod_{j=1,l,L} \mathrm{d}W_j(\alpha_j), \tag{19}$$

where $\mathrm{d}W_j(\alpha_j)$ is given by

$$\mathrm{d}W_j(\alpha_j) = \mathrm{d}M_j^2 A_{ex}(M_j)A_{st}(\alpha_j)A_{qs}(\alpha_j)\mathrm{d}R_{n_j}(M_j;\alpha_j) \prod_{i=1}^{n_j} \mathrm{d}m_i F_i(m_i). \tag{20}$$

In (19), the square of the CM energy of the projectile-cluster interaction is related to the four-momentum p_L of the residual nucleus according to

$$s' = (p - p_L)^2, \tag{21}$$

and the factor $A_{sc}(t')$ describes the deflection of the projectile and the cluster in dependence on the four-momentum t' transferred in the projectile-cluster collision. The invariant masses of the excited projectile, cluster and residual nucleus are denoted by M_1, M_l and M_L. The factors $A_{ex}(M_j)$, $A_{st}(\alpha_j)$ and $A_{qs}(\alpha_j)$ describe the excitation of the subsystems and the statistical properties of the final states into which the excited subsystems decay. A detailed discussion of these factors for hadrons and clusters can be found in [22]. Each subsystem is characterized by two parameters. The "temperature" parameter – denoted by $(\Theta_1, \Theta_l, \Theta_L)$ for the three subsystems under consideration – determines the excitation energy, while the volume parameter (R_1, R_l, R_L) is responsible for the particle density at the break-up point. In (20), the mass of a produced resonance is described by a Breit-Wigner distribution $F_i(m_i)$ with position and width taken from [35], while for a stable particle $F_i(m_i)$ represents a δ function. The treatment of the residual nucleus is based on the same principal assumptions used for hadrons and clusters and is fully described in [13].

All calculations in this paper are carried out using the following set of parameters independent of energy and target mass:

$$\begin{aligned} R_1 &= 1.2 \text{ fm} \quad \Theta_1 = 300 \text{ MeV} \\ R_l &= 1.2 \text{ fm} \quad \Theta_l = 100 \text{ MeV} \\ R_L &= 1.7 \text{ fm} \quad \Theta_L = 5 \text{ MeV} \left[1 - \exp\left(-l/3\right)\right]. \end{aligned} \tag{22}$$

The dependence of the temperature Θ_L of the target residue on the number l of participants will be discussed in the next subsection.

3.3. Comparison of the folding and the ROC model

In the framework of the ROC model any physical quantity is calculated as a sum over the contributions from collisions of the projectile with different numbers of participating nucleons. The first two items of this sum, the interaction with one and two participants, are related to the first-collision model (8) and the two-step reaction mechanism (14). The similiarity is quite obvious in the case of one participating nucleon, where only the implementation of the elementary cross section differs. In the folding model a parametrization taken from experimental results is applied, in the ROC model the calculation of the elementary cross section is an inherent constituent of the model itself.

In the case of two participating nucleons the folding model in the form applied here assumes that there is a pion in the intermediate state. It would be consistent to take into account all intermediate particle species compatible with quantum number conservation. This is difficult to realize, because

the corresponding elementary cross sections are unknown in many cases. Therefore, the ROC model avoids the detailed dynamical description of the various two-step processes but instead calculates the statistical weights of all possible final channels. Analogous discussions hold for the similiarity between three (and more)-step mechanisms and reactions with three (and more) participants.

While the ROC model takes into account the kinetic and excitation energy of the residual nucleus, the folding model completely neglects the target residue. This may be less important at high energies, but in the threshold region the folding-model results should be considered rather as an upper limit. By the folding procedures (8) and (14) with the off-shell treatment of all particles the Fermi motion is used to gain the energy necessary for particle production. However, the kinetic and excitation energy carried away by the residual nucleus may considerably influence the energy balance of the whole pA interaction.

In the folding model final-state interaction is accounted for via multiplying the K^--production cross section with a reabsorption factor κ which is definded in terms of the K^-N cross section and deduced from geometrical considerations. In the ROC model the temperature Θ_L of the residual nucleus is, according to (22), proposed to increase if the number of participants l becomes larger. The more target nucleons participate in the interaction, the more particles traverse the residual nucleus and the more secondary interactions take place. Thus, FSI is taken into account in a global and averaged manner simply by giving the residual nucleus a temperature without distinguishing between the various processes caused by the different particle species. This global way of treating FSI will be contrasted in the following section with the quite different method applied for the folding-model calculations.

4. Final-state interactions

The strong effect of FSI on K^- production in heavy-ion collisions was discussed by Zwermann and Schürmann [20], Ko [36] and Barz and Iwe [37]. Due to the large K^-N cross section the produced antikaons are rescattered by the surrounding nuclear matter. In addition to the possibility of elastic scattering, K^- mesons may be absorbed via the reaction $K^- + N \rightarrow \Lambda + \pi$. It was found by Cugnon et al. [38] and Gibbs and Kruk [39] that K^- absorption is the dominant reaction mechanism for hyperon production in antiproton-nucleus annihilation at rest. Detailed calculations and the comparison with extensive experimental data obtained in $\bar{p}A$ annihilations showed that K^- mesons interact with nuclear matter according to the free K^-N cross section. In Fig. 3 we show the total and inelastic K^-N cross sections calculated by parametrizations suggested in [38]. The parameters were obtained by fitting the experimental data from compilation [40].

Ko [36] assumed that also the contribution from the $\Lambda(1520)$ resonance is important to account for FSI. Due to its narrow width and, therefore, the long lifetime, $\Lambda(1520)$ decays outside the target nucleus. However, nothing is known about the $\Lambda(1520)N$ interaction and, what is even more important, for kinematical reasons the probability to form such

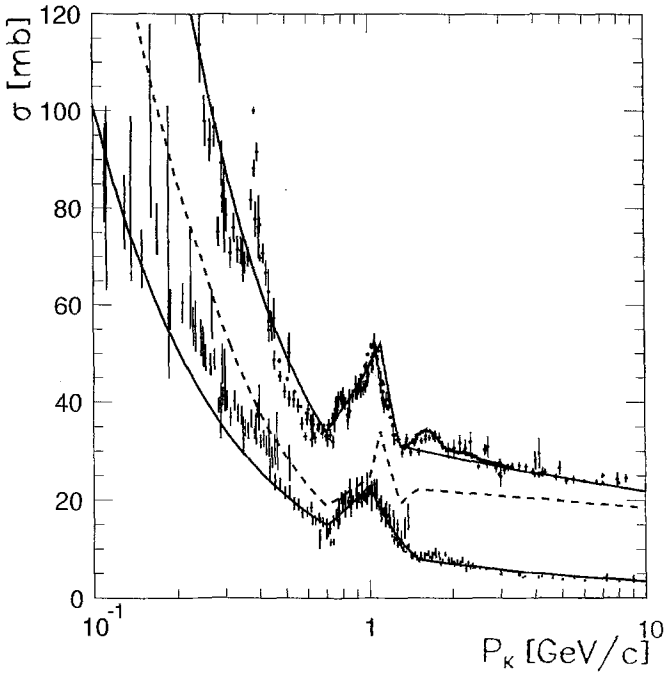

Fig. 3. Total (*upper solid line*), elastic (*lower solid*) and inelastic (*dashed*) K^-N cross section as a function of the kaon momentum [38, 41]. The experimental data points are taken from [40]

a narrow resonance is negligible. For this reason we consider only non-resonant K^-N interactions and assume that the cross section in nuclear matter equals the free one in accordance with [38, 39].

The inelastic mean free path of a K^- meson in nuclear matter is $\lambda = (\sigma_{KN}\rho_0)^{-1}$, where σ_{KN} is the inelastic K^-N cross section and ρ_0 is the average nuclear density of about 0.16 fm^{-3}. The average K^--meson collision number then is $n_K \simeq R/\lambda$, with R being the radius of the interaction zone. We consider only inelastic K^-N interactions in order to evaluate the K^- reabsorption, although elastic K^-N collisions may also change the shape of observed distribution [36]. The standard way [11, 20, 36, 37] to account for particle reabsorbtion in pA and AA collisions is to multiply the production cross section by the factor

$$\kappa(p_{K^-}, A) = \exp(-n_K), \quad n_K = \rho_0 \sigma_{KN}(p_{K^-}) R(A). \quad (23)$$

In accordance with [11] it is assumed that the radius of the interaction zone equals the nuclear radius $R = r_0 A^{1/3}$ with r_0=1.2 fm. Reabsorption factors calculated with (23) for Be and Pb targets and for two values of the K^-N cross section are shown in Table 1. For a lead target the reabsorption factor is about 0.2 for K^- mesons with momenta $p_{K^-} > 500\,\mathrm{MeV/c}$ ($\sigma_{KN} \simeq 20$ mb) and reaches a value of ~0.01 for soft antikaons ($\sigma_{KN} \simeq 40$ mb). It was estimated by Zwermann and Schürmann [20] that the suppression factor for K^- production in SiSi collisions is about 0.3. Even for a Be target soft kaons are strongly reabsorbed.

In Table 1 we also show the K^--reabsorption factor calculated according to the assumption of a uniform distribution of the produced antikaons inside the target nucleus

$$\kappa(p_{K^-}, A) = \frac{\pi \rho_0 r_0^3}{n_K} \quad (24)$$

Table 1. K^--reabsorption factors calculated for Be and Pb targets and for two values of σ_{KN}

	σ_{KN}=20 mb		σ_{KN}=40 mb	
Function	Be	Pb	Be	Pb
(23)	0.45	0.2	0.1	0.01
(24)	0.67	0.46	0.34	0.18
(25)	0.79	0.67	0.097	0.084

$$\left\{1 - \frac{1}{2n_K{}^2}\left[1 - (1 + 2n_K)\exp(-2n_K)\right]\right\}.$$

It should be noted that Parametrization (24) is based on the Glauber approach, i.e. on the assumption that the produced particles propagate through the nucleus on a straight line. Consequently, the reabsorption factor (24) may only be used when the mean free path $(\sigma_{KN}\rho_0)^{-1}$ of the K^- mesons is larger than the nuclear radius ($p_{K^-} > 2$ GeV/c for a ^{12}C nucleus). Nevertheless, in Table 1 we also show the results calculated with (24) in order to compare the different models accounting for FSI. It is obvious that reabsorption factor (24) strongly differs from assumption (23), especially for heavy targets. Recently, a simple model for particle reabsorption in nuclei at intermediate energies was developed by Vercellin et al. [42] for the description of η production in nuclei [43]. The results from [42] practically coincide with (24).

To understand the discrepancy we made calculations with the cascade model COMIC described in detail in [44]. We performed the calculations for Be, Al, Cu, Sn, Ta and Pb targets and for various values of σ_{KN}. The factor κ obtained from the cascade calculations can be parametrized as follows

$$\kappa(p_{K^-}, A) = (3.9 - 0.024 \times \sigma_{KN})A^{-2/3}\ , \qquad (25)$$

where σ_{KN} is in mb. The cascade results for Be and Pb targets are also shown in Table 1. In this case, the mass dependence is much smaller than for the two other approaches.

The effect of FSI of produced K^- mesons with the residual nucleus is strong for soft kaons and heavy targets. Moreover, as can be seen from Table 1, there are considerable discrepancies between the different descriptions of the K^- reabsorption. In order to get a better understanding of the problem it is necessary to study the A dependence of K^- production both for low- and high-momentum kaons.

The K^- meson is an excellent probe to study the properties of strongly interacting particles in nuclear matter whereas for example the analysis of η-meson FSI seems to be quite difficult because of the uncertainty in the ηN cross section due to the influence of the $N^*(1535)$ resonance. The K^-N cross section is experimentally well known. Thus, the study of K^- production with $p_{K^-} < 500$ MeV/c where σ_{KN} is large (see Fig. 3) is very interesting. It seems useful to test the K^+K^--pair production in nuclei for this purposes. Whereas K^- mesons strongly interact with the surrounding nuclear matter, the K^+ mesons escape the interaction zone due to the small K^+N cross section. Consequently, the investigation of the dependence of the K^+K^--pair production on the target mass will be a good tool for analyzing K^- reabsorption.

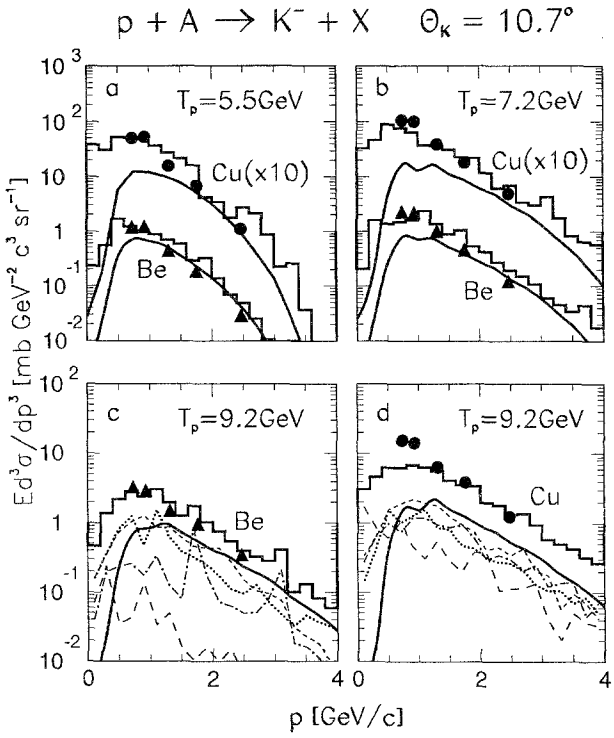

Fig. 4a–d. Momentum spectra of K^- mesons measured in pBe and pCu collisions under 10.7° at proton energies **a** T_p = 5.5 GeV, **b** T_p = 7.2 GeV **c** and **d** T_p = 9.2 GeV. The experimental data (*circles*) from [45] are compared with the results from the ROC- (*histograms*) and the folding-model (*solid lines*) calculations. In (**c**) and (**d**) the *dashed, dotted, dash-dotted* and *long-dashed lines* represent the ROC-model results with one to four participants, respectively

5. Comparison with experimental data

5.1. Momentum spectra

Calculations in the framework of the folding and the ROC model are compared with experimental data on K^- production in proton-nucleus collisions above the NN threshold. In the calculations with the folding model only the direct K^- production (8) is taken into account, since the two-step reaction mechanism is assumed to contribute mainly in the threshold region. The justification of this assumption will be discussed in Sect. 6.

The following analysis of the experimental data covers projectile energies from 5.5 to ~14 GeV in which the elementary K^--production cross section (7) calculated with the ROC model and Parametrization (6) used in the folding model are similar. To estimate the effect of FSI K^- reabsorption is taken into account in the folding-model calculations by using (23) because this parametrization seems most reasonable for the description of the propagation of fast and slow hadrons through nuclei and is quite frequently used in calculations of pA and AA collisions [11, 26, 46].

Recently, the production of K^- mesons in collisions of protons with Be, Al, Cu and Ta targets at incident energies 5.5, 7.2 and 9.2 GeV and an emission angle of 10.7° has been studied at the ITEP proton synchrotron [45]. In Fig. 4a–d the model calculations are compared with the experimental results from pBe and pCu collisions. While the ROC model reasonably describes the experimental data on

invariant cross sections of K^- production, the folding model underestimates the data from the copper target in the low-momentum region. In order to understand this discrepancy the ROC-model contributions from the partial processes with one, two, three and four participants are displayed [see (17)]. There is a remarkable agreement between the one-participant contribution from the ROC model and the direct production mechanism calculated in the framework of the folding model. This result confirms the conjecture from Sect. 3.3 about the similiarity in the description of the one-participant and the direct production mechanism. In the case of the Be target the contributions from the higher order processes with more than one participant are small and both the folding and the ROC model yield a reasonable description of the spectrum. The situation changes, however, if the target becomes heavier. Then the probability for higher order processes increases and their consideration is mandatory to achieve a good reproduction of the spectrum.

Figure 5 shows the invariant cross sections of K^- production in pBe and pCu collisions measured at 3.5° and a projectile energy of 9.2 GeV. The agreement between the experimental data and the calculated results is rather good for both models. A comparison of Fig. 4c,d with Fig. 5a,b shows that the folding model describes the momentum spectra at 3.5° much better than at 10.7°. Since the estimate of the reabsorption according to (23) is independent of the emission angle, this fact indicates a stronger angular dependence of the folding-model results than observed experimentally. An explanation can be found by looking again at the partial processes. The higher-order processes contribute less at the smaller angle, and the error caused by their neglection in the folding model is not so important. In view of these results an extension of the investigation to a broader angular region would be worthwhile. Obviously, the neglection of higher order processes in the folding model should be restricted to light targets and small angles.

In Fig. 6 the spectra of K^- mesons measured by the E802 Collaboration [3] at BNL in pBe and pAu collisions at 14.6 GeV/c are shown. The invariant cross sections are plotted as a function of $T_t = m_t - m_K$, where $m_t = (p_t^2 + m_K^2)^{1/2}$ is the transverse mass, p_t the transverse momentum and m_K the K^- mass. The spectra were integrated over a rapidity range of $1.2 \leq y \leq 1.4$. The folding model reasonably reproduces the spectra from the Be target but underestimates the results from the Au target. The calculations with the ROC model describe the K^- spectra quite well both for Be and Au targets, although there is a tendency to overestimate the cross section at high momenta in the case of the Be target.

It should be emphasized that the E802 data are reproduced by calculations made in the framework of standard reaction mechanisms. There seems to be no room for exotic reaction mechanisms such as quark-gluon plasma formation, at least in the case of proton-induced reactions.

5.2. *A dependence of K^- production*

The dependence of strange-particle yields on the size of the colliding nuclei is frequently discussed as one of the most promising ways to search for quark-qluon plasma formation [3, 7, 48]. Singh [48] discussed the dependence of the

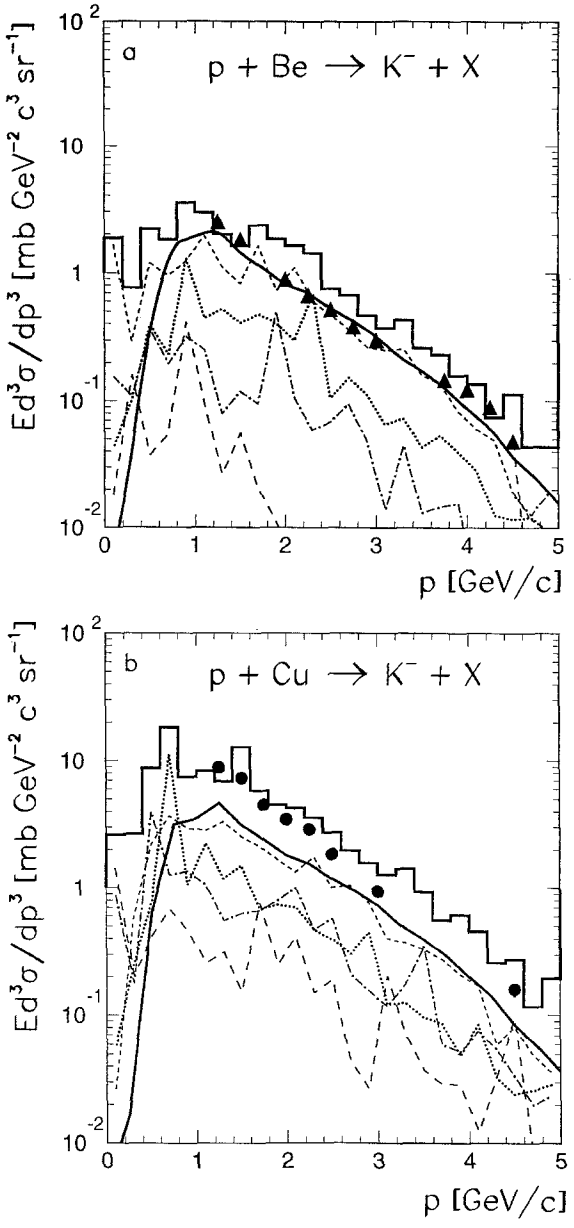

Fig. 5. Same as Fig. 4 for $T_p = 9.2$ GeV and a kaon-emission angle 3.5°. Experimental data are taken from [46]

K^+/K^- ratio on the size of AA systems, while the A dependence of K^+ production in pA collisions at high energies ($s > 20$ GeV^2) was studied both experimentally and theoretically in [46, 47, 49].

The dependence of the invariant cross section of K^- production on the target mass A can be factorized in the following way:

$$E_{K^-} \frac{\mathrm{d}^3\sigma_{K^-}}{\mathrm{d}\mathbf{p}_{K^-}} = g(p_t, x_R, s) \times A^{\alpha(x_R)}. \tag{26}$$

To compare the data obtained at different collision energies it is convenient to describe the exponent α as a function of the radial scaling variable x_R. It was found that the experimental data are reasonably reproduced by (26) and, moreover, at high collision energies ($s > 20$ GeV^2) the parameter α neither depends on s nor on the kind of the observed

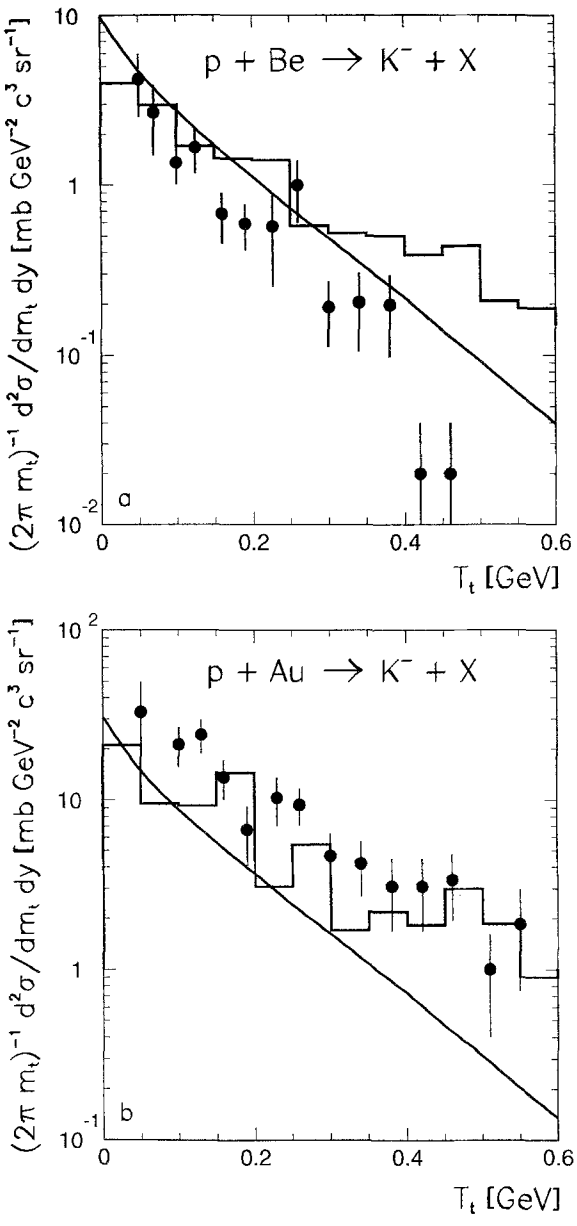

Fig. 6. Invariant cross section for K^- production in (**a**) pBe and (**b**) pAu collisions as a function of the transverse kinetic energy T_t. The rapidity range is $1.2 \leq y \leq 1.4$. The experimental data (*circles*) are from [3]. The histograms show the ROC-model and the solid lines the folding-model results

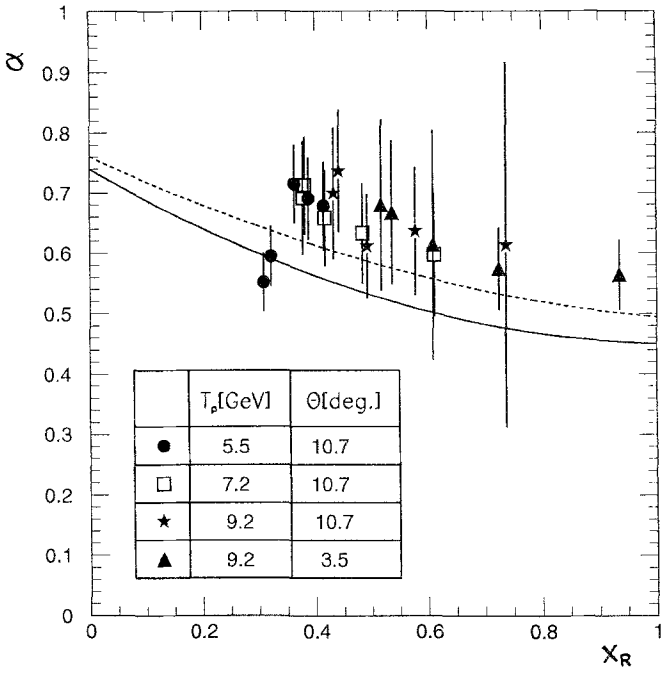

Fig. 7. Parameter α describing the A dependence of K^- production as a function of the radial scaling variable x_R. The *data points* represent the experimental results for different proton energies T_p and kaon-emission angles. The *solid line* shows the fit (27) to experimental data obtained at 100 GeV [47]. The *dashed line* shows the ROC-model results

hadron. This fact is frequently denoted as the A universality of proton-nucleus collisions.

In Fig. 7 the $\alpha(x_R)$ dependence extracted from the whole set of the experimental data [45, 46] is shown. Each α value is obtained by fitting (26) to the four experimental data points from the targets Be, Al, Cu and Ta for given incidence energy, emission angle and K^--meson momentum. The error bars are too large to establish significant dependences on x_R, bombarding energy and emission angle. The mean value of all points is equal to 0.65 indicating an A dependence of the cross section which is in accordance with the geometrical cross section.

The same procedure is carried out with the results from the ROC-model calculations. All obtained α values are then fitted with a quadratic function on x_R represented by the dashed line in Fig. 7. For comparison the function

$$\alpha(x_R) = 0.74 - 0.55x_R + 0.26x_R^2 \qquad (27)$$

obtained by Barton et al. [47] in an analysis of the A dependence of p, π^+, π^-, K^+, K^- and $\bar{p}$ production in pA collisions at an incident proton energy of 100 GeV is drawn as a solid line. From the remarkable agreement between the various results shown in Fig. 7 it can be concluded that the A universality of pA collisions originally observed at high energies is valid also at the relatively low energies ($s \leq 14$ GeV^2) considered in this paper.

In the folding model the A dependence is defined by two factors [see (8)]: the first one is the effective nucleon number N_{eff} which scales like $A^{0.79}$. The second factor is related to K^- FSI and may be evaluated from (23), (24) or (25). To analyze the A dependence of K^- production on FSI it is convenient to use the following definition

$$A^\alpha \propto N_{\text{eff}} \times \kappa(p_{K^-}, A) \propto A^{0.79} \times A^{\alpha_{\text{FSI}}}, \qquad (28)$$

where the coefficient α_{FSI} accounts for FSI of the K^- with the residual nucleus. With an experimental value of $\alpha \simeq 0.65$ and using (28) we expect a reabsorption coefficient of

$$\alpha_{\text{FSI}} \simeq 0.65 - 0.79 = -0.14\ . \qquad (29)$$

In the following we will compare the value of the coefficient $\alpha_{\text{FSI}} = -0.14$, which is expected from the analysis of the experimental data [see Fig. 7 and (28)], with those calculated using the different approaches (23), (24) or (25). Note that all experimental values were obtained for K^- momenta $p_{K^-} > 0.75$ GeV/c or $\sigma_{KN} = 20$ mb.

The cascade model [see (25)] predicts $\kappa \propto A^{-2/3}$ and, therefore, a coefficient $\alpha_{\text{FSI}} \simeq -0.67$ which is significantly different from -0.14.

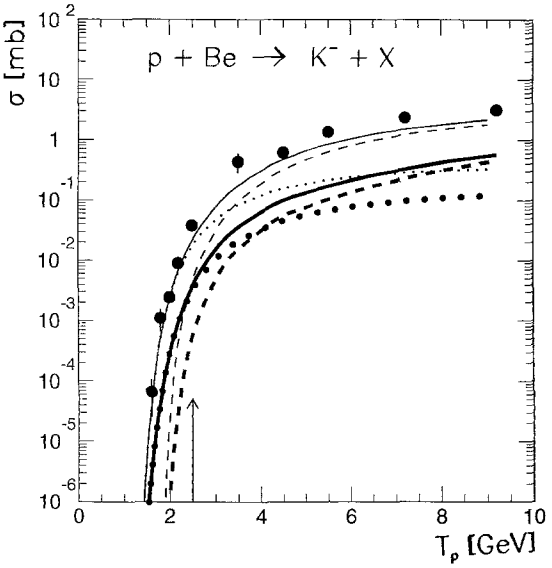

Fig. 8. Total K^--production cross section in pBe collisions as a function of the kinetic proton energy T_p. The *points* show the ROC-model and the lines the folding-model results. The folding-model calculations are shown for direct (*dashed line*) and two-step (*dotted*) reactions and the sum of both mechanisms (*solid*). The effects of FSI are included (*thick lines*) and switched off (*thin lines*) in the folding-model calculations. The *arrow* indicates the NN threshold

Parametrization (23) defines the following A dependence

$$\alpha_{\mathrm{FSI}} = -\frac{\sigma_{KN}\rho_0 r_0 A^{1/3}}{\ln A}, \tag{30}$$

where notations are taken from (23). It follows that $\alpha_{\mathrm{FSI}} \simeq -0.4$ for σ_{KN}=20 mb. Obviously, (23) predicts a reabsorption factor which is in contradiction with the experimental results.

In order to evaluate the A dependence of the reabsorption factor from (24) and $\sigma_{KN} \simeq$20 mb the numerical results calculated with (24) are fitted in the same way as the experimental data. It is found that $\alpha_{\mathrm{FSI}} \simeq -0.19$ which is closer to the expected value of -0.14. However, as discussed above the applicability of (24) to heavy nuclei where $(\sigma_{KN}\rho)^{-1} < R$ is questionable.

Summarizing, the A dependence of K^- production in pA reactions seems to be most sensitive to distinguish between different models for final-state interactions. The discussed parametrizations of FSI cannot satisfactorily reproduce the A dependence of the available data. Further systematical theoretical as well as experimental studies especially at low K^- momenta where σ_{KN} is large are needed.

6. K^- production at threshold

Theoretical studies of K^+ and η meson production in proton-nucleus collisions [11, 12, 27, 43] show that, in the framework of the folding model, secondary processes ($p + N \rightarrow \pi + X, \pi + N \rightarrow K^+$ or $\eta + X$) mainly contribute at bombarding energies below the reaction threshold s_{th} for the free NN interaction. In the framework of multi-particle collision models it is assumed that at subthreshold energies the particles are produced via the interaction of the incident proton

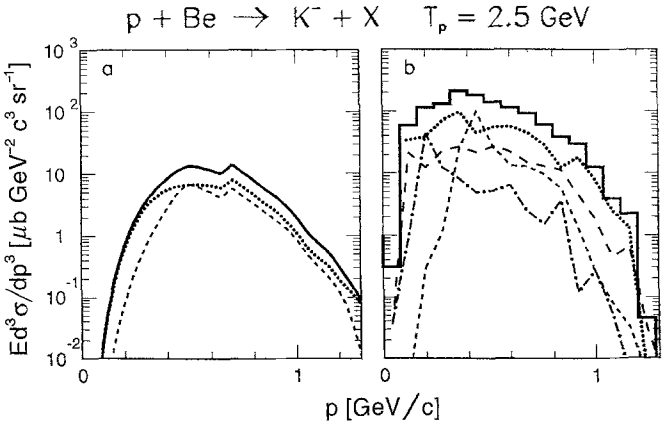

Fig. 9. Folding-model (**a**) and ROC-model (**b**) predictions for the K^--momentum spectra produced in pBe collisions at T_p = 2.5 GeV integrated over kaon-emission angles $0° \leq \theta \leq 10°$. In (**a**) the *dashed* and *dotted lines* represent the results for the direct (8) and the two-step (14) mechanism. In (**b**) the *dashed, dotted, dash-dotted* and *long-dashed lines* represent the processes with one, two, three and four participants. The *thick solid line* and the *thick histogramm* are the sums of the partial processes

with several target nucleons [13]. In both approaches the basic idea to explain subthreshold particle production is concerned with the implementation of nuclear medium effects.

The K^--production cross section in pBe collision is calculated using the ROC and the two variants of the folding model, the direct production (8) and the two-step process (14). Since the K^- FSI is smaller for light nuclei, we restrict our considerations to the Be target in order to reduce the uncertainties connected with the treatment of FSI. The K^- reabsorption is taken into account in the folding-model calculations using (23).

In Fig. 8 the ROC-model results (full circles) are plotted as a function of the projectile energy T_p. All results are obtained using the same set [see (22)] of parameters. However, as discussed in [13], the temperature Θ_L of the target residue may become a function of the incidence energy at low energies. This can considerably influence the calculated cross sections. An increase of the temperature decreases the cross section and vice versa. Therefore, the displayed results should be considered as an estimate for the order of magnitude especially at the lowest energies.

The folding-model result for direct K^- production is shown by the thick dashed line in Fig. 8. The disagreement between the ROC and the folding model is mainly caused by differences in the elementary cross section σ_{KN} for K^- production. In the folding-model calculations Parametrization (6) is used giving cross sections which are about one order of magnitude smaller than those predicted by the ROC model at collision energies close to threshold ($s - s_{\mathrm{th}} < 0.1$). In addition, different methods are applied concerning the treatment of K^- reabsorption and energy absorption by the target residue. These differences are significant even for energies $T_p > 4$ GeV, mainly because of the strong reabsorption of slow antikaons. It was found from the comparison with the experimental data in Sect. 5 that calculations with the folding model taking into account FSI according to (23) did not reproduce K^- spectra from pBe interactions at low momenta. This leads to the underestimation of the

total production-cross section by an order of magnitude in comparison with the ROC-model results. At subthreshold energies FSI of K^- mesons is even more significant, because the antikaons are produced with small momenta. To test the validity of this argumentation we make calculations with the folding model taking σ_{K^-} from (7) and assuming $\kappa(p_{K^-}, A) = 1$. The result, shown in Fig. 8 by the thin dashed line, reasonably agrees with the ROC-model calculations at energies above 3 GeV. However, in the subthreshold region the difference between the ROC- and folding-model result for direct production remains, which may be due to the contribution from the two-step reaction mechanism.

By the thick dotted line in Fig. 8 we show the folding-model results for the two-step processes (4), (14) with FSI (23), whereas by the thin dotted line the result with $\kappa(p_{K^-}, A) = 1$ is displayed. Noticeably the contribution from the two-step reaction mechanism becomes dominant at incident proton energies below 4 GeV. Moreover, the sum of the K^--production cross sections calculated for direct and two-step processes nearly equals the ROC-model result if FSI is neglected in the folding-model calculations (thin solid line). This finding reflects the fact that the ROC model takes into account the contributions from all possible channels of K^- production in pA collisions.

It seems promising to study the non-direct reaction mechanism of K^- production in pA collisions at bombarding energies $T_p \leq 4$ GeV. At subthreshold energies the contribution from secondary processes becomes dominant. Obviously, at threshold energies the produced K^- mesons are forward peaked and can be studied with the 0° Facility at COSY-Jülich [8]. In Fig. 9 the K^--momentum spectra from pBe collisions at 2.5 GeV as predicted by the folding and the ROC model are compared. The results differ by about one order of magnitude. This gives an impression of the uncertainties which must be managed when preparing an experiment on K^- production in this energy region. According to the folding model comparable contributions from the direct (8) and the two-step (14) mechanism are expected, while the ROC model predicts considerable contributions even from processes with three and four participants.

The K^- mesons are produced with momenta below 1 GeV/c, where σ_{KN} is large (see Fig. 3). Therefore, the study of the K^- production at threshold energies gives the opportunity to analyze the strong FSI as discussed in Sect. 4 as well as the influence of higher-order processes with more than two participants.

7. Summary

We study the production of K^- mesons in proton-nucleus collisions at bombarding energies up to ~15 GeV. The elementary cross section σ_{K^-} for the reaction $p+p \rightarrow K^- + X$ is analyzed and parametrizations of σ_{K^-} are compared with the available experimental data. We calculate σ_{K^-} with the Rossendorf Collision (ROC) model and get a reasonable description of the data as well as a prediction of the K^--production cross section at near-threshold energies, where so far no data are available.

The principal assumptions of the ROC model and the folding model are described. Because of the large cross section the K^- strongly interact with the surrounding nuclear matter. We discuss the FSI of produced K^- mesons with the residual nucleus and evaluate the effective reabsorption factor. We found that the different approaches [11, 42, 44] for the description of particle reabsorption in nuclei are in strong contradiction with each other. The advantages of using K^- mesons for studing the problem is discussed.

The calculations with the ROC and folding model are compared with experimental data on differential cross sections of K^- production in pA collisions [25, 45, 46]. The ROC model reproduces momentum spectra and A dependence, while the folding model fails in describing the A dependence. It was found that the observed discrepancy is obviously due to the treatment of K^- reabsorption. In the analysis of the measured A dependence of K^- production different methods of taking FSI into account are considered. It was found that (24) gives the best results but its applicability is questionable.

We discuss the K^- production in pA collisions at energies close to the reaction threshold where the contribution from secondary processes may be evaluated. These processes also seem to be responsible for strangeness production in heavy-ion collisions at high energies, because of the large pion multiplicity [6, 7]. We find that the study of the K^--production mechanism in pA interactions, which is important in view of understanding the heavy-ion collision dynamics and discussions about the signatures of the quark-gluon plasma, is also very informative at incident proton energies below 4 GeV. We propose to study the $p + A \rightarrow K^- + X$ reaction at threshold collision energies at COSY-Jülich using the 0° Facility where K^- mesons under forward angles can be detected.

Acknowledgement. The authors acknowledge stimulating discussions with V. Komarov, O.W.B. Schult and K. Sistemich throughout the course of this study.

References

1. Rafelski, J., Müller, B.: Phys. Rev. Lett. **48**, 1066 (1982)
2. Greiner, C., Koch, P., Stöcker, H.: Phys. Rev. Lett. **58**, 1825 (1987)
3. Abbott, T., Akiba, Y., Beavis, D., et al.: Phys. Rev. Lett. **66**, 1567 (1991)
4. Helios Collaboration: Nucl. Phys. A **525**, 227c (1991)
5. Bartke, J., Bialkowska, H., Bock, R., Brockmann, R., Chase, S.I.: Z. Phys. C **38**, 191 (1990)
6. Stachel, J.: Nucl. Phys. A **527**, 167 (1991)
7. Nagamiya, S.: Nucl. Phys. A **544**, 5c (1992)
8. Borgs, W., Büscher, M., Gotta, D., et al.: COSY Proposal 18 Jülich 1990
9. Kilian, K., Machner, H., Oelert, W., et al.: COSY Proposal 15 Jülich 1990
10. Chumakov, M., Kiselev, Y., Martemyanov, A., Mikhailov, K., Sheinkman. V.: ITEP Proposal Moscow 1993
11. Cassing, W., Batko, G., Mosel, U., Niita, K., Schult, O., Wolf, G.: Phys. Lett. B **238**, 25 (1990)
12. Sibirtsev, A.A., Büscher, M.: Z. Phys. A **347**, 191 (1994)
13. Müller, H., Sistemich, K.: Z. Phys. A **344**, 197 (1992)
14. Sibirtsev, A.A.: Sov. J. Nucl. Phys. **55**, 145 (1992)
15. Reed, J.T., Melissinos, A.C., Reay, N.W., Yamanouchi, T., Sacharidis, E.J., Lindenbaum, S.J., Ozaki, S., Yuan, C.L.: Phys. Rev. **168**, 1495 (1968)

16. Louttit, R.I., Morris, T.W., Rahm, D.C., Rau, R.R., Thorndike, A.M., Willis, W.J., Lea, R.M.: Phys. Rev. **123**, 1465 (1961)
17. Efremov, S.V., Paryev, E.Y.: Yad. Fiz. **57**, 563 (1994)
18. Flaminio, V., Moorhead, W.G., Morrison, D.R.O., Rivoire, N.: Compilation of cross sections. CERN-HERA 84-01 (1984) Geneva
19. Giacomelli, G.: Int. J. Mod. Phys. A **5**, 223 (1990)
20. Zwermann, W., Schürmann, B.: Phys. Lett. B **145**, 315 (1984)
21. Efremov S.V., Kazarnovsky, M.V., Pariev, E.Y., : Z. Phys. A **344**, 181 (1992)
22. Müller, H.: Z. Phys. A **336**, 103 (1990)
23. Wroblewski, A.: Acta Phys. Pol. B **16**, 379 (1985)
24. Müller, H.: Proc. 105th International WE-Heraeus-Seminar "Hadronic Processes at Small Angles in Storage Rings" (1993) Rössle, E., Schult, O.W.B. (eds.) p. 117
25. Shor, A., Ganezek, K., Abachi, S., Carroll, J., Geaga, J., et al.: Phys. Rev. Lett. **48**, 1597 (1982)
26. Li, G.Q., Ko, C.M., Fang, X.S.: Phys. Lett. B **329**, 149 (1994)
27. Cassing, W., Batko, G., Vetter, T., Wolf., G.: Z. Phys. A **340**, 51 (1991)
28. Sibirtsev, A.A.:Acta Phys. Pol. B **24**, 1849 (1993)
29. Glauber, R.J., Mathiae, J.: Nucl.Phys. B **21**, 135 (1970)
30. Taylor, F.E., Carey, D.C., Johnson, J.R., et al.: Phys. Rev. D **14**, 1217 (1976)
31. Johnson, J.R., Kammerud, R., Ohsugi, T., et al.: Phys. Rev. D **17**, 1292 (1978)
32. Anisovich, V.V., Shekhter, V.M.: Nucl. Phys. B **55**, 455 (1973)
33. Müller, H.: Z. Phys. A **339**, 409 (1991)
34. Byckling, E., Kajantie, K.: Particle kinematics, New York, London, Sydney 1973, Wiley
35. Hernández, J.J., Stone, J., Porter, F.C., et al.: Phys. Lett. B **239**, 1 (1990)
36. Ko, C.M.: Phys. Lett. B **138**, 361 (1984)
37. Barz, H.W., Iwe, H.: Phys. Lett. B **153**, 217 (1985)
38. Cugnon, J., Deneye, P., Vandermeulen, J.: Phys. Rev. C **41**, 1701 (1990)
39. Gibbs, W.R., Kruk, J.W.: Phys. Lett. B **237**, 317 (1990)
40. Flaminio, V., Moorhead, W.G., Morrison, D.R.O., Rivoire, N.: Compilation of cross sections. CERN-HERA 83-02 (1983) Geneva
41. Cugnon, J.: Private communication
42. Vercellin, E., Chiavassa, E., Dellacasa, G., et al.: Nuovo Cimento A **106**, 861 (1993)
43. Chiavassa, Dellacasa, G., De Marco, N., et al.: Z. Phys. A **344**, 345 (1993)
44. Sibirtsev, A.A.: Sov. J. Nucl. Phys. **55**, 729 (1992)
45. Lepikhin, Y., Pasko, S., Smirnitsky, A., Sheinkman, V.: Sov. J. Nucl. Phys. (to be published)
46. Sibirtsev, A.A., Vorontsov, I.A., Safronov, G.A., Smirnov, G.N., Trebuchovsky, Y.V.: Sov. J. Nucl. Phys. **51**, 1001 (1990)
47. Barton, D.S., Brandenburg, G.W., Busza, W., et al.: Phys. Rev. D **27**, 2580 (1983)
48. Singh, C.P.: Phys. Rep. **236**, 175 (1993)
49. Abe, F., Hara, K., Kim, N., et al.: Phys. Rev. D **30**, 1861 (1984)